

Magneto-elastic coupling between copper spin configurations and oxygen octahedra in $\text{La}_{2-x}\text{Sr}_x\text{CuO}_4$. Untwinning, Raman (phonon) spectrum, and neutron response

Marcello B. Silva Neto¹

¹*Institute for Theoretical Physics, University of Utrecht,
Leuvenlaan 4, 3584 CE Utrecht, The Netherlands.*

We reinterpret neutron scattering and Raman spectroscopy experiments in $\text{La}_{2-x}\text{Sr}_x\text{CuO}_4$, showing modulation of spin and lattice degrees of freedom both in the low-temperature orthorhombic and tetragonal phases, in terms of a magneto-elastic coupling between noncollinear configurations for the copper spins and the oxygen octahedra. The magneto-elastic coupling furthermore explains the recently discovered magnetic-field induced untwinning in $\text{La}_{2-x}\text{Sr}_x\text{CuO}_4$, for $x < 2\%$, and allows us to understand why in $\text{La}_{2-x-y}\text{Nd}_y\text{Sr}_x\text{CuO}_4$ with $y = 0.4$ and $x = 1/8$, for example, when (1,0) and/or (0,1) static spin spirals are stabilized due to hole frustration, the atomic modulation in the low-temperature tetragonal phase of $\text{La}_{2-x-y}\text{Nd}_y\text{Sr}_x\text{CuO}_4$ has a periodicity of 4 lattice spacings, half the magnetic one.

PACS numbers: 74.25.Ha, 75.10.Jm, 74.72.Dn

I. INTRODUCTION

$\text{La}_{2-x}\text{Sr}_x\text{CuO}_4$ is one of the best studied high temperature superconductors and is a system where the phenomenon of 1D charge segregation, or stripes formation, has been argued to occur¹. In fact, inelastic neutron scattering experiments within the superconducting phase of $\text{La}_{2-x}\text{Sr}_x\text{CuO}_4$, $x > 5.5\%$, have revealed that dynamical incommensurate (IC) spin correlations coexist with superconductivity². In addition, it has also been observed experimentally the existence of IC "charge" peaks accompanying the IC magnetic order (even though neutrons cannot directly probe charge distributions), with twice the incommensurability of the magnetic one. This phenomenon is most clearly observed when a low-temperature tetragonal (LTT) phase is stabilized, for example by Nd doping,¹ and it was immediately interpreted as an evidence of the formation of charge stripes that act as antiphase domain walls.³ In the same spirit, the observation of *diagonal* static IC magnetic correlations at even lower doping, $2\% < x < 5.5\%$, within the low-temperature orthorhombic (LTO) spin-glass (SG) phase of $\text{La}_{2-x}\text{Sr}_x\text{CuO}_4$,⁴ as well as recent evidence of diagonal "charge" modulation from Raman spectroscopy,⁵ have also been used to support the picture of *diagonal* stripe formation at lower doping.

In this article we propose an alternative interpretation for the above described experimental results as originating from a magneto-elastic coupling between the Cu^{++} spins and the lattice in $\text{La}_{2-x}\text{Sr}_x\text{CuO}_4$.⁶ We start by explaining the recently discovered magnetic-field induced untwinning in $\text{La}_{2-x}\text{Sr}_x\text{CuO}_4$.⁷ According to Ref. 7, the two inequivalent orthorhombic directions of La_2CuO_4 can be swapped at room temperature by the application of a strong in-plane magnetic field, $B \sim 14$ T. This remarkable effect was confirmed by X-ray measurements showing changes in the structure of $\text{La}_{2-x}\text{Sr}_x\text{CuO}_4$, and the crystallographic rearrangement observed in an optical microscope.⁷ This effect has been used since then to pro-

duce extremely high quality untwinned $\text{La}_{2-x}\text{Sr}_x\text{CuO}_4$ single crystals. We then argue that it is precisely this same magneto-elastic coupling that gives rise to a supermodulation of the oxygen octahedra when a noncollinear configuration for the Cu^{++} magnetic moments is stabilized, as a consequence of the magnetic frustration introduced by hole-doping,⁸ and we discuss its effects on the Raman and neutron responses, for the case of noncollinear magnetic structures both within the LTO and LTT phases of $\text{La}_{2-x}\text{Sr}_x\text{CuO}_4$.

II. THE MAGNETO-ELASTIC COUPLING

In La_2CuO_4 each Cu^{++} ion is located at the center of an oxygen octahedron, see Fig. 1. The crystal field produced by the O^{--} ions of the octahedron splits the energy levels of the Cu^{++} orbitals in such a way that the unpaired electron is found at the $d_{x^2-y^2}$ orbital. This is a planar orbital located at the base of the octahedron (the common base of its two pyramids). The spin-orbit (SO) interaction in La_2CuO_4 then introduces a large XY anisotropy that favors a configuration for the Cu^{++} spins parallel to the plane of the $d_{x^2-y^2}$ orbital. In case there is no tilting of the octahedra, this corresponds to confining the spins to the CuO_2 layers, as it happens for example in the $\text{Sr}_2\text{CuO}_2\text{Cl}_2$ system. On the other hand, for La_2CuO_4 the tilting of the oxygen octahedra in the LTO phase generates a Dzyaloshinskii-Moriya interaction that determines an easy-axis for the antiferromagnetic ordering and leads to the canting of the spins out of the CuO_2 planes, see Fig. 1. This can be better understood by using the notation introduced in Ref. 9. We first write the spin of Cu^{++} in terms of its staggered, \mathbf{n} , and uniform, \mathbf{L} , components, $\mathbf{S}_i/S = e^{i\mathbf{Q}\cdot\mathbf{x}_i}\mathbf{n}(\mathbf{x}_i) + \mathbf{L}(\mathbf{x}_i)$, where, as usual, $\mathbf{Q} = (\pi, \pi)$ is the antiferromagnetic ordering wave vector. Then we introduce a thermodynamic Dzyaloshinskii-Moriya vector \mathbf{D}_+ pointing along the axis of tilting of the oxygen octahedra, see Fig. 1.

The magnetic free-energy density for uniform configurations of the staggered moments in a single layer of La_2CuO_4 is⁹

$$\mathcal{F}_M = \frac{1}{2gc} \{ (\mathbf{n} \cdot \mathbf{D}_+)^2 + \Gamma_{XY} n_c^2 + (\mathbf{n} \cdot \mathbf{B})^2 - 2\mathbf{B} \cdot (\mathbf{n} \times \mathbf{D}_+) \}, \quad (1)$$

where $gc = 8Ja^2$, Γ_{XY} is the XY anisotropy energy, J is the in-plane antiferromagnetic superexchange, and a is the lattice spacing. We now introduce a lattice free-energy density

$$\mathcal{F}_L = -\zeta \mathbf{D}_+ \cdot \hat{\mathbf{X}}, \quad (2)$$

which favours \mathbf{D}_+ oriented along a certain direction $\hat{\mathbf{X}}$ in a fixed laboratory reference frame. The parameter ζ introduced here controls the softness of the oxygen octahedra and in the case $\zeta \rightarrow \infty$ the octahedra becomes completely rigid and fixed to the laboratory frame.

Since the orientation of \mathbf{D}_+ defines the local orthorhombic coordinate system of the crystal, we conclude that, at zero magnetic field, $\mathbf{B} = 0$, the equilibrium configuration of the system is such that $\mathbf{D}_+ \parallel a \parallel \hat{\mathbf{X}}$ with

$$\mathbf{n}(\mathbf{x}_i) \cdot \mathbf{D}_+ = 0, \quad \text{and} \quad \mathbf{L}(\mathbf{x}_i) = \frac{1}{2J} (\mathbf{D}_+ \times \mathbf{n}(\mathbf{x}_i)). \quad (3)$$

Together with the large XY anisotropy, which confines $\mathbf{n}(\mathbf{x}_i)$ to the orthorhombic ab basal-plane, the above two conditions uniquely determine the easy-axis and canting of the Cu^{++} spins, with $\mathbf{n} \parallel b$ and $\mathbf{L} \parallel c$, see Fig. 1.

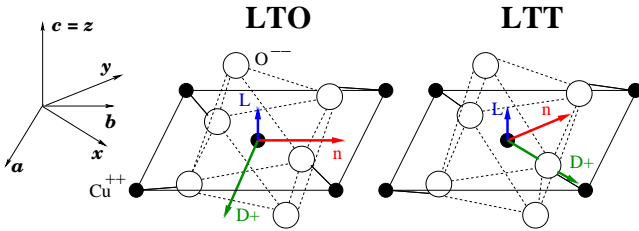


FIG. 1: (Color online) Left: LTO (abc) and LTT (xyz) coordinate systems. Center and Right: Tilting of the octahedron in the LTO (center) and LTT (right) phases. Uniform spin component \mathbf{L} (blue arrow), staggered spin component \mathbf{n} (red arrow), and Dzyaloshinskii-Moriya vector \mathbf{D}_+ (green arrow).

III. MAGNETIC UNTWINNING

The physics of the magneto-elastic coupling in $\text{La}_{2-x}\text{Sr}_x\text{CuO}_4$ is essentially given by Eqs. (1) and (3). These equations imply that the vectors \mathbf{n} , \mathbf{L} , and \mathbf{D}_+ , form a triad of vectors mutually orthogonal that can only move rigidly, see Fig. 1. Let us now consider twins A and B such that the orthorhombic basis-vectors in twin A are rotated by $\pi/2$ relative to the ones in twin B,

$\hat{\mathbf{X}}_A \perp \hat{\mathbf{X}}_B$, see Fig. 2. When a strong in-plane magnetic field, $B > 2gc\zeta$, is applied parallel to the $\hat{\mathbf{X}}_A$ orthorhombic direction of twin A, we find that the total free energy $\mathcal{F}_M + \mathcal{F}_L$ is minimized, within such twin domain, for a new configuration of \mathbf{n} and \mathbf{D}_+ such that $\mathbf{n} \parallel c_A$ and $\mathbf{D}_+ \parallel b_A$ (see Fig. 2, middle panel). This is only possible if accompanied by a $\pi/2$ rotation of the entire octahedra in twin A (remember that \mathbf{D}_+ determines the axis of the tilting of the octahedra), which then causes the swap of the local orthorhombic directions. In twin B the effect of the same magnetic field is harmless, since it is longitudinal, $\mathbf{B} \perp \hat{\mathbf{X}}_B$. In fact, a longitudinal magnetic field in La_2CuO_4 causes a continuous rotation of the two vectors, \mathbf{n} and \mathbf{L} , within the bc plane,^{10,11} as a result of the term $-2\mathbf{B} \cdot (\mathbf{n} \times \mathbf{D}_+)$ in Eq. (1). Since in twin B the \mathbf{D}_+ vector remains perpendicular to the bc plane, such rotation can take place without causing structural changes. When the field is removed, \mathbf{n} and \mathbf{L} return to their original positions (as originally in twin B), but the orthorhombic axis in twin A remain swapped.

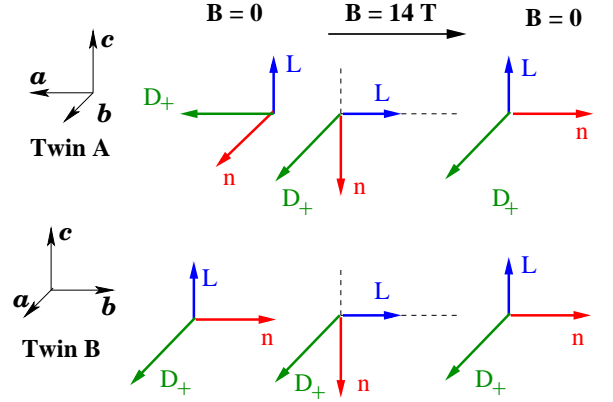


FIG. 2: (Color online) i) $\mathbf{B} = 0$ (left): the two twins have basis-vectors rotated by $\pi/2$ relatively; ii) $\mathbf{B} = 14$ T: the basis-vectors in twin A swap due to the flop of staggered field \mathbf{n} and orient identically to the ones of twin B, where the staggered \mathbf{n} and uniform \mathbf{L} vectors are rotated in the bc plane (see discussion in the text); iii) $\mathbf{B} = 0$ (right): the staggered \mathbf{n} and uniform \mathbf{L} vectors return to their equilibrium positions and the crystal remains untwined.

The important message from this magneto-elastic allowed untwining in $\text{La}_{2-x}\text{Sr}_x\text{CuO}_4$ is that *a change in the spin configuration can have a strong effect on the equilibrium position of the tilting axis of the oxygen octahedra*. What is most surprising, however, are the associated energy scales, especially being an effect originated from SO coupling. Besides the ability of causing the swap of the crystallographic axis in a magnetic field (the sample actually expanded about 1% along the orthorhombic b direction after the untwining⁷) magnetic susceptibility experiments in $\text{La}_{2-x}\text{Sr}_x\text{CuO}_4$ by Lavrov *et al.*,¹² at much lower fields, have shown that the Cu^{++} spins remain confined to the orthorhombic (bc) plane, for different doping concentrations, $0 < x < 4\%$, and for a rather

wide temperature range, $0 < T < 400$ K.¹² This is another consequence of Eqs. (3) that dictates that the \mathbf{n} and \mathbf{D}_+ vectors should be perpendicular.⁹ In what follows we shall discuss the effects of the magneto-elastic coupling on the oxygen octahedra and its effect on the Raman and neutron responses, for the case of noncollinear magnetic structures both within the LTO and LTT phases.

IV. RAMAN SPECTRUM IN THE LTO PHASE

In a recent publication,¹³ it was shown that the magnetic frustration introduced by hole-doping in the LTO phase of $\text{La}_{2-x}\text{Sr}_x\text{CuO}_4$ gives rise, above a certain critical doping, to a static helicoidal supermodulation where the \mathbf{n} vector precesses (in space) around the b easy-axis

$$\mathbf{n}(\mathbf{x}_i) = (\sigma_a \cos(\mathbf{Q}_S \cdot \mathbf{x}_i), n_b(\mathbf{x}_i), \sigma_c \sin(\mathbf{Q}_S \cdot \mathbf{x}_i)), \quad (4)$$

with the wave vector for the spin incommensurability $\mathbf{Q}_S \parallel b$, $\sigma_c \ll \sigma_a \ll 1$, and $n_b^2 = 1 - n_a^2 - n_c^2$.¹³ Such helicoidal structure was then shown to be consistent with the magnetic susceptibility experiments in $\text{La}_{2-x}\text{Sr}_x\text{CuO}_4$ for $x = 2\%, 3\%$ and 4% , since it guarantees that the total magnetization in a applied field remains confined to the bc plane.¹³

The physical picture behind the formation of such helicoidal structure can be easily understood as follows. Above a certain critical doping, that is essentially determined by the strength of the Dzyaloshinskii-Moriya gap, $\Delta_{DM}/J \sim 0.02$, the magnetic frustration introduced by the doped-holes favours a noncollinear configuration for the Cu^{++} spins. Since these are coupled to the oxygen octahedra by the magneto-elastic coupling in Eq. (3), any spin rotation should be accompanied by a rotation of the tilting axis of the octahedra (\mathbf{D}_+ is now $\mathbf{D}_+(\mathbf{x}_i)$). However, in the LTO phase of $\text{La}_{2-x}\text{Sr}_x\text{CuO}_4$, there are no n -fold axis of rotation with $n > 2$, and thus the orthorhombicity frustrates any such rotation. For example, the in-plane spiraling of the \mathbf{n} vector is forbidden because it would require a continuous rotation of the tilting axis of the octahedra around the c axis and this is not allowed in the LTO phase. Thus, for Sr concentration well above the critical doping, deep inside the SG phase, the resulting noncollinear spin structure in the LTO phase corresponds to, for example, a helicoidal modulation of the \mathbf{n} vector around the b easy-axis, as in Eq. (4), accompanied by a precession of the octahedron around its equilibrium ($x = 0$) position, see Fig. 3. Furthermore, such atomic modulation has wave vector for atomic incommensurability given by $\mathbf{Q}_C \parallel b$.

It is worth pointing out that, for even lower doping, $x \approx 0.01, 0.024$, it has been recently shown by Luscher *et al.*¹⁴ that the appropriate noncollinear spin structure is such that the \mathbf{n} field instead oscillates within the CuO_2 plane around the b easy-axis. We emphasize here that, once the magneto-elastic coupling in Eq. (3) is taken into account, such oscillation also gives rise to a modulation of the octahedra, just as in the case of the helicoid.

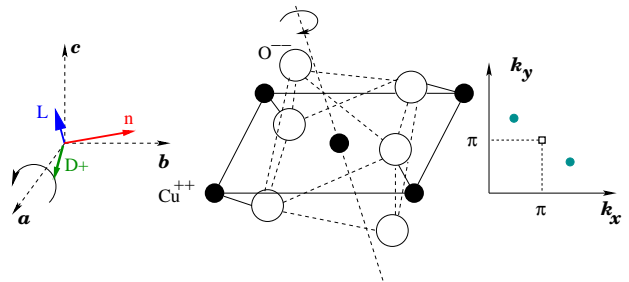


FIG. 3: (Color online) Precession of the triad (left) and octahedron (center) around their equilibrium ($x = 0$) position. The precession takes place as one goes along the b axis, such that the two wave vectors \mathbf{Q}_S and \mathbf{Q}_C are parallel to b . Right: neutron response in the LTO phase due to modulation of \mathbf{n} . The neutron response is shifted from the Néel peak (unfilled square at (π, π)) to new diagonal incommensurate positions (filled circles), due to the helicoidal magnetic modulation described by Eq. 4.

The magnetic modulation with wave vector $\mathbf{Q}_S \parallel b$, either helicoidal¹³ or oscillatory¹⁴, gives rise to the diagonal IC peaks observed in the neutron response,⁴ see Fig. 3. A supermodulation of the octahedron, in turn, would result in the appearance of a plethora of extra vibrational modes that could be accessed via Raman spectroscopy.¹⁶ As we shall now demonstrate, this is actually the case. On the top of Fig. 4, $x = 0$, we observe 5 sharp phonon peaks, corresponding to the symmetric vibrational modes predicted by group theory and accessible in the (AA) (red-solid-curve) and (BB) (blue-dashed-curve) Raman geometries. We also observe a sharp B_{1g} phonon signal at 220 cm^{-1} , accessible in the (BA) (black-dotted-curve) geometry. As doping concentration is increased, $x = 1\%$ and 3% , the 5 sharp phonon peaks are replaced by much more numerous and broader ones while the B_{1g} phonon remains sharp, although with decreasing intensity, see Fig. 4. This is a consequence of the enlargement of the atomic unit cell associated with the supermodulation of the octahedra with wave vector $\mathbf{Q}_C \parallel b$ (\mathbf{Q}_C is the wave vector for the modulation of $\mathbf{D}_+(\mathbf{x}_i)$), see Fig. 3.

In fact, recent Raman experiments in $\text{La}_{2-x}\text{Sr}_x\text{CuO}_4$ at $x = 2\%$ showed indications of anisotropic atomic modulation in the B_{2g} Raman geometry.⁵ These results are consistent with the above physical picture of the octahedra supermodulation. The atomic modulation resulting from the precession of the octahedra has wave vector $\mathbf{Q}_C \parallel b$. In order to probe such modulation, we must choose a Raman geometry such that the wave vector \mathbf{Q}_C has a finite projection on the axis of the electric field of both incoming e_{in} and outgoing e_{out} light. Thus, the above octahedra supermodulation should become accessible exactly in the B_{2g} geometry, where e_{in} and e_{out} are oriented along the Cu-Cu bonds, with respect to which \mathbf{Q}_C is diagonal.⁵ Furthermore, it should not be accessible at all in the (BA) geometry (black-dotted-curve)

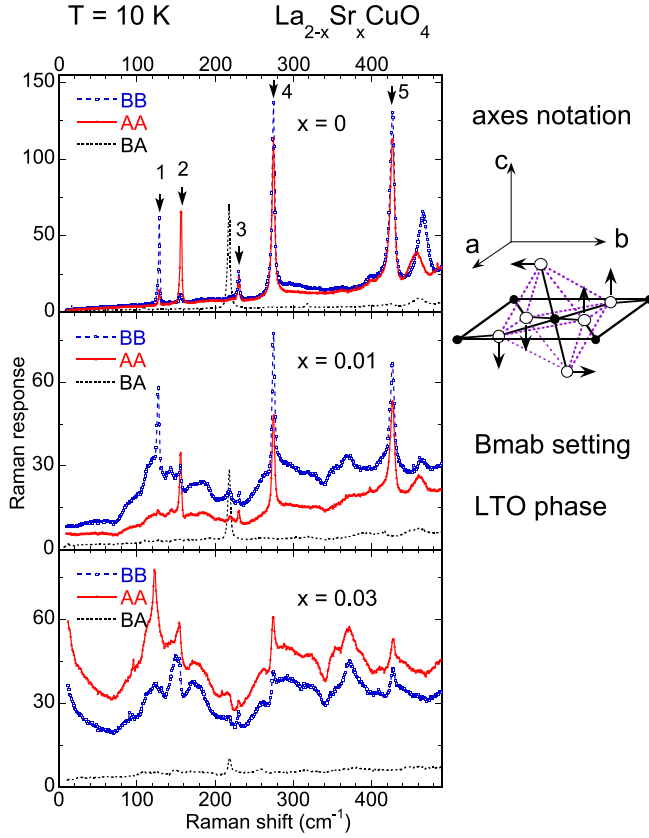


FIG. 4: (Color online) Raman response at 10 K in the (AA) (red-solid), (BB) (blue-dashed), and (BA) (black-dotted) polarization configurations, for $x = 0, 1\%$, and 3% (from Ref. 16). For $x = 0$ we clearly see sharp phonon peaks corresponding to the 5 symmetric Raman active modes predicted by group theory, as well as one B_{1g} phonon. For $x = 1\%$ and 3% , however, a larger number of peaks is observed, signaling the enlargement of the atomic unit cell.

where e_{in} and e_{out} are oriented along the orthorhombic basis-vectors, and this results in a rather featureless B_{1g} response (except for the phonon at 220 cm^{-1}), see Fig. 4. Although the results by Tassini *et al.*⁵ were interpreted as a signature of diagonal stripe formation, we believe that the octahedra supermodulation provides a more reasonable explanation for the Raman response reported in Fig. 4 and in Ref. 5, especially for the $x = 1\%, 3\%$ samples where stripes can be safely ruled out.

V. NEUTRON RESPONSE IN THE LTT PHASE

When a tetragonal phase is stabilized in $\text{La}_{2-x}\text{Sr}_x\text{CuO}_4$, by Nd doping for example, incommensurate "charge" peaks are observed in neutron scattering, whose incommensurability is twice the magnetic one, see Fig. 5. Even though neutrons cannot directly couple to charge excitations, this result has been

interpreted, for over 10 years, as a sign of charge stripe formation acting as anti-phase domain walls.

Let us now demonstrate how the magneto-elastic Eqs. (3) can be used to explain the neutron scattering results within the LTT phase. In the LTT phase, the \mathbf{D}_+ vector points along one of the basal tetragonal directions, say x , such that two oxygen atoms remain confined to the tetragonal basal plane while the other two are tilted, one above and one below the CuO_2 layers, see Fig. 1. From the magneto-elastic coupling equations Eq. (3) we then find $\mathbf{n} \parallel y$ and $\mathbf{L} \parallel z$. There is one major difference, however, regarding possibilities for the rotation of the tilting axis of the octahedron between the LTO and LTT phases when a noncollinear spin structure is favoured. In the LTT phase, the z axis is in fact a n -fold axis with $n > 2$, and a in-plane rotation of the staggered moments is now not only allowed but energetically favourable (as discussed earlier, the XY anisotropy favours $\mathbf{n}(\mathbf{x}_i)$ to be parallel to the planes). The above argument is consistent with the calculations by Sushkov and Kotov,¹⁵ using realistic parameters for the $t-t'-t''-J$ model, which showed that the magnetic ground state, in the LTT phase, is composed by $(1, 0)$ and/or $(0, 1)$ spirals

$$\mathbf{n}(\mathbf{x}_i) = (\cos(\mathbf{Q}_S \cdot \mathbf{x}_i), \sin(\mathbf{Q}_S \cdot \mathbf{x}_i), 0), \quad (5)$$

with $Q_S = \delta \sim x$. The magneto-elastic coupled spiraling of the Cu^{++} spins and tilting axis of the octahedra, \mathbf{D}_+ , produces the pattern depicted in Fig. 5.

Now, by analyzing Fig. 5 we can finally understand why the atomic incommensurability is twice the magnetic one, and why for $x = 1/8$ the atomic periodicity is of 4 lattice spacings. Since $Q_S = \delta \sim x$, for $x = 1/8$ the spin periodicity is of 8 lattice spacings, obtained after 8 rotations of $\pi/4$.¹⁵ However, after 4 rotations of $\pi/4$, when the spins are anti-parallel, the configuration of the octahedron is equivalent to the initial one, see Fig. 5. Although this might not be apparent on a first inspection due to the difference in the tilting of the oxygen atoms, we should not forget that in a body-centered tetragonal unit cell, such as the one of $\text{La}_{2-x}\text{Sr}_x\text{CuO}_4$, corner and central Cu^{++} ions are equivalent. Thus, any symmetry operation can be defined together with a half translation of the lattice vectors. This brings the octahedron on the far right of Fig. 5 to the one in the far left, and so they are indeed equivalent. Notice now that the modulation of the atoms in the octahedra is half the magnetic one, and so the neutron response in the reciprocal space should be such that the atomic incommensurability is twice the magnetic one,¹ see Fig. 5.

Finally, the magneto-elastic coupling might also gives us a hint towards the understanding of some unexpected features on the phonon spectrum of the $\text{La}_{2-x-y}\text{Nd}_y\text{Sr}_x\text{CuO}_4$ system, at $x = 1/8$ and $y = 0.4$, recently reported by the Raman experiments of Gozar *et al.* in Ref. 16. It has been observed that the lowest energy of the A_g phonon modes, there denoted A mode, has a rather broad Raman spectral line. Since this is the phonon mode related to the spatial distribution of

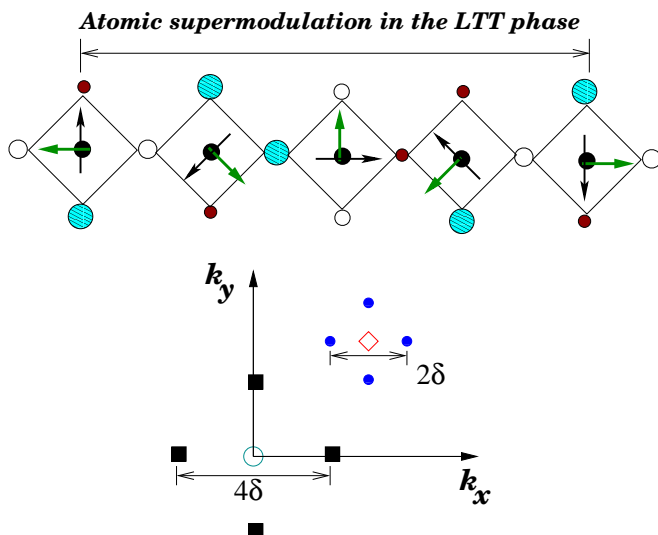


FIG. 5: (Color online) Top: Magneto-elastic coupled spiraling of the Cu^{++} spins (black arrows, V-shaped tip) and \mathbf{D}_+ (green arrow, triangular tip). Blue (larger and hatched) oxygen atoms are canted up the plane, red (smaller and filled) ones are canted down the plane, and open ones are confined to the basal plane. The octahedra on the far left and far right, exactly at half the magnetic periodicity, are equivalent (see discussion in the text). Bottom: Since the atomic periodicity is half the magnetic one, the neutron response in reciprocal space is such that the atomic incommensurability (large filled squares) is twice the magnetic one (smaller filled circles).

the tilting angle of the oxygen octahedra, the Raman data seems to indicate a locally fluctuating octahedra tilt distribution in $\text{La}_{2-x-y}\text{Nd}_y\text{Sr}_x\text{CuO}_4$,¹⁶ that can be understood in terms of short-range magneto-elastic coupled spin-tilt-axis fluctuations.

VI. CONCLUSIONS

We have shown that neutron scattering and Raman spectroscopy experiments, either in the LTO or LTT phases of $\text{La}_{2-x}\text{Sr}_x\text{CuO}_4$, as well as the process of untwining in a strong in-plane magnetic field, can be understood in terms of the unusually strong magneto-elastic coupling between the noncollinear configuration for the Cu^{++} spin and the oxygen octahedra. Although the analysis here performed can go no further than discussing static phenomena of charge and spin ordering, it is very much possible that the distribution of oxygen doped holes in $\text{La}_{2-x}\text{Sr}_x\text{CuO}_4$ will follow the anisotropic 1D octahedra modulation proposed above, thus presenting us with an interesting possibility for the origin of the anisotropic 1D electronic (charge) dynamics in cuprates. This interesting possibility is presently under investigation.¹⁷

VII. ACKNOWLEDGEMENTS

The author acknowledges invaluable discussions with Y. Ando, L. Benfatto, A. H. Castro Neto, B. Keimer, A. Gozar, C. Morais Smith, and O. Sushkov. A special thanks goes to A. Gozar for kindly producing Fig. 4, containing the data published in Ref. 16.

- ¹ J. M. Tranquada, B. J. Sternlieb, J. D. Axe, Y. Nakamura, and S. Uchida, *Nature (London)* **375**, 561 (1995).
- ² K. Yamada, C. H. Lee, K. Kurahashi, J. Wada, S. Wakimoto, S. Ueki, H. Kimura, Y. Endoh, S. Hosoya, G. Shirane, R. J. Birgeneau, M. Greven, M. A. Kastner, and Y. J. Kim, *Phys. Rev. B* **57**, 6165 (1998).
- ³ J. Zaanen and O. Gunnarsson, *Phys. Rev. B* **40**, 7391 (1989); K. Machida, *Physica C* **158**, 192 (1989).
- ⁴ S. Wakimoto, G. Shirane, Y. Endoh, K. Hirota, S. Ueki, K. Yamada, R. J. Birgeneau, M. A. Kastner, Y. S. Lee, P. M. Gehring, and S. H. Lee, *Phys. Rev. B* **60**, 769(R) (1999); S. Wakimoto, R. J. Birgeneau, M. A. Kastner, Y. S. Lee, R. Erwin, P. M. Gehring, S. H. Lee, M. Fujita, K. Yamada, Y. Endoh, K. Hirota, and G. Shirane, *Phys. Rev. B* **61**, 3699 (2000); M. Fujita, K. Yamada, H. Hiraka, P. M. Gehring, S. H. Lee, S. Wakimoto, and G. Shirane, *Phys. Rev. B* **65**, 064505 (2002).
- ⁵ L. Tassini, F. Venturini, Q.-M. Zhang, R. Hackl, N. Kikugawa, and T. Fujita, *Phys. Rev. Lett.* **95**, 117002 (2005).
- ⁶ M. A. Kastner, R. J. Birgeneau, G. Shirane, and Y. Endoh, *Rev. Mod. Phys.* **70**, 897-928 (1998).
- ⁷ A. N. Lavrov, S. Komiya, and Y. Ando, *Nature* **418**, 385 (2002).
- ⁸ B. I. Shraiman and E. D. Siggia, *Phys. Rev. B* **46**, 8305

- (1992).
- ⁹ M. B. Silva Neto, L. Benfatto, V. Juricic, and C. Morais Smith, *Phys. Rev. B* **73**, 045132 (2006).
- ¹⁰ M. B. Silva Neto and L. Benfatto, *Phys. Rev. B* **72**, 140401(R) (2005).
- ¹¹ M. Reehuis, C. Ulrich, K. Proke, A. Gozar, G. Blumberg, Seiki Komiya, Yoichi Ando, P. Pattison, and B. Keimer, *Phys. Rev. B* **73**, 144513 (2006).
- ¹² A. N. Lavrov, Yoichi Ando, Seiki Komiya, and I. Tsukada, *Phys. Rev. Lett.* **87**, 017007 (2001).
- ¹³ V. Juricic, M. B. Silva Neto, and C. Morais Smith, *Phys. Rev. Lett.* **96**, 077004 (2006).
- ¹⁴ A. Lüscher, G. Misguich, A. I. Milstein, and O. P. Sushkov, *Phys. Rev. B* **73**, 085122 (2006).
- ¹⁵ O. P. Sushkov and V. K. Kotov, *Phys. Rev. B* **70**, 024503 (2004); *Phys. Rev. Lett.* **94**, 097005 (2005).
- ¹⁶ A. Gozar, Seiki Komiya, Yoichi Ando, and G. Blumberg, in *Magnetic and Charge Correlations in $\text{La}_{2-x-y}\text{Nd}_y\text{Sr}_x\text{CuO}_4$: Raman Scattering Study*, Frontiers in Magnetic Materials (Ed. A.V. Narlikar), Springer-Verlag Berlin Heidelberg, pp. 755-789 (2005).
- ¹⁷ M. B. Silva Neto, in preparation.